ISSN 0208-7774 TRIBOLOGIA 1/2017 p. 97–104

Mariusz WALCZAK[*], Maciej ZWIERZCHOWSKI[**], Jarosław BIENIAŚ[*], Jacek CABAN[***]

THE TRIBOLOGICAL CHARACTERISTICS OF Al-Si/GRAPHITE COMPOSITE

CHARAKTERYSTYKA TRIBOLOGICZNA KOMPOZYTU Al-Si/GRAFIT

Key words: aluminium matrix composite, graphite, sliding friction, wear testing.

Abstract: The paper presents the results of tribological research on AlSi12CuNiMg/5.7 wt.% Gr aluminium composite material (containing graphite particles in the amount of 5.7% wt.%) and on its matrix. This composite is used as high-tech construction material in the automotive industry, particularly for pistons, cylinder liners, and slide bearings. The tribological properties of these materials can be significantly changed as a result of the introduction of graphite particles. Therefore, wear tests have been carried out using the ball-on-disc tribometer. Microstructure and wear resistance of the matrix and composite alloy have been subjected to comparative analysis. It was demonstrated that the composite reinforced with graphite is characterized by a lower friction coefficient and lower wear in comparison to the matrix.

Słowa kluczowe: aluminiowe materiały kompozytowe, grafit, tarcie ślizgowe, testy zużycia.

Streszczenie: Artykuł przedstawia wyniki badań tribologicznych aluminiowego materiału kompozytowego AlSi12CuNiMg/5.7 wt.% Gr (zawierającego cząsteczki grafitu w ilości 5,7% wag.) i jego osnowy. Kompozyt ten znajduje zastosowanie jako nowoczesny materiał konstrukcyjny w przemyśle motoryzacyjnym, szczególnie na tłoki, tuleje cylindrowe i łożyska ślizgowe. Wprowadzenie cząstek grafitu znacząco może zmieniać właściwości tribologiczne tych materiałów. W tym celu wykonano testy zużycia na tribometrze typu kula-tarcza. Mikrostruktura i odporność na zużycie stopu osnowy i kompozytu zostały poddane analizie porównawczej. Wykazano, że kompozyt zbrojony grafitem charakteryzuje się mniejszym współczynnikiem tarcia i mniejszym zużyciem w porównaniu z osnową.

INTRODUCTION

Al-Si cast alloys are very popular in the transport industry due to their numerous attractive features, e.g., high strength to low specific gravity ratio, the low value of thermal expansion, excellent castability, and corrosion resistance **[L. 1]**. Al-Si eutectic alloys (i.e. AlSi12CuNiMg) are mainly used in the automotive industry for the manufacturing of pistons, cylinder liners, connecting rods, and engine blocks **[L. 2, 3]**.

Recently Aluminium Matrix Composites (AlMC) reinforced with fine ceramic graphite particles, fly ash, SiC, and Al_2O_3 particles are increasingly gaining in importance in the scope of scientific research works and in implementation activities **[L. 4–6]**.

From among the wide spectrum of metal composite materials, the materials based on the system consisting of aluminium alloy – graphite particles (Al/Gr) deserve a special mention. Excellent physicochemical and operational properties are achieved thanks to the presence of dispersed graphite particles in aluminium matrix **[L. 7]**.

Moreover, the presence of solid, soft, and lubricating graphite particles in aluminium matrix leads to the significant improvement of anti-seizing properties and to better vibration damping **[L. 7, 8]**. The anti-

[*] Lublin University of Technology, Faculty of Mechanical Engineering, Department of Materials Engineering, 36 Nadbystrzycka Street, 20-618 Lublin, Poland, e-mails: m.walczak@pollub.pl, j.bienias@pollub.pl.

[**] Wrocław University of Technology, Faculty of Mechanical Engineering, Institute of Production Engineering and Automation, 5 Łukasiewicza Street, 50-371 Wrocław, Poland, e-mail: maciej.zwierzchowski@pwr.wroc.pl

[***] University of Life Sciences in Lublin, Faculty of Production Engineering, Department of Transporting and Agricultural Machinery, 28 Głęboka Street, 20-612 Lublin, Poland, e-mail: jacek.caban@up.lublin.pl

seizing properties of Al/Gr composites are particularly important in the case of cold engine starting or the lack of proper lubrication.

Casted pistons of compression-ignition (Diesel) engines made of Al-Si/Gr composites reduce the value of specific fuel consumption by 3% and the value of engine power losses caused by friction by 9% in comparison to applied conventional aluminium alloys of cast iron **[L. 9]**. It is possible due to the presence of lubricating graphite layer, high vibration damping capability, and the low value of thermal expansion coefficient. The high vibration damping capability of Al-Si/Gr pistons eliminates the piston slap and piston ring clearance as well as maintains a continuous hydrodynamic oil coating, reducing the friction between piston ring and sleeve surface as well as reducing the wearing of piston rings **[L. 10, 11]**.

Aluminium is characterized by significant reactivity and by the local increase of mating elements temperature in the course of sliding resulting in surface oxidation **[L. 10, 12]**.

Investigations **[L. 13]** on the impact of Si content on wear in aluminium casting alloys indicated that abrasion wear occurs at a Si content of 12%. The authors emphasize that mainly two abrasive wear mechanisms are present in such case: (1) ploughing action in the case of alloys subjected to heat treatment and (2) the combination of ploughing action and cutting in the case of alloys not subjected to heat treatment. Furthermore, they show that nucleation of Al alloy cracks takes place mainly on the Al/Si contact surface due to the high stress concentration on the interface between Si particles and Al matrix. Needle-shaped eutectoid Si will easily lead to the nucleation and propagation of cracks. This state is eliminated by the spheroidization of eutectic silicon as a result of heat treatment.

In the course of the analysis of abrasive wear in eutectic Al-Si alloys, Mahato et al. **[L. 14]** observed Si decohesion from the matrix resulting in the occurrence of regional cracks. In all probability, this process is facilitated by high velocities of deformation in sub-surface regions, and it causes the accumulation of dislocations on Si borders. Furthermore, the increasing occurrence of brittle oxides is observed in the region of micro-cracks occurrence due to increased oxygen diffusion.

In the opinion of Omrani et al. **[L. 10],** graphite particles reduce the value of shear stress and plastic deformations in sub-surface area performing the role grease between the both slipping surfaces.

Rajaram et al. **[L. 15]** indicate that wear progress in Al-Si/Gr composites takes place through the creation of sub-surface cracks, which locate at the previous location of separated Si particles in matrix alloy due to high shear stress. The wear is determined by occurring delaminations and the coalescence of these cracks. Then the wear process is carried out in the form of the removal of successive layers of material as a result of the delamination of sub-surface layers.

The application of aluminium alloy - graphite particles in combustion engines elements, e.g., cylinder liners, significantly reduces their wear, improves the efficiency, increases the engine power, and reduces operation costs. The reduction of losses caused by friction between the piston and cylinder liner can significantly contribute to the increase of mechanical efficiency **[L. 11]**.

The cylinder liners used by Honda Corporation (staple fibre 12% Al_2O_3, 9% graphite) are integrated with the cylinder block. The thickness of friction layer has been reduced to 2/3 in comparison to previously used aluminium alloy and the previous mass was maintained. However, the mass has been reduced by 50% in comparison to cast iron inserts. Cooling effectiveness has been improved in a significant manner **[L. 16]**.

The bearings characterized by lower weight, self-lubricating, and generating lower production costs in comparison to currently manufactured bearings, e.g., made of copper, lead, tin, and cadmium alloys can prove to be the most promising application of casted Al/Gr composites **[L. 8]**.

The friction joint and particularly the type of directly contacting materials are important in tribological processes. The knowledge of tribological characteristics and wearing mechanisms is essential in the course of designing, selection of materials and in the course of the selection of machine parts production technology. Therefore, the purpose of the research was to determine the impact of reinforcing layer (in the amount of 5.7 wt.% graphite) on wearing in dry sliding condition in regards to matrix alloy AlSi12CuNiMg.

MATERIAL AND METHODS

AlSi12CuNiMg casting aluminium alloy reinforced with fine graphite particles in the amount 5.7 wt.% has been used in tests. AlSi12CuNiMg/5.7 wt.% Gr composite was manufactured in the Foundry Research Institute in Cracow in the gravity casting process. Graphite particles coated with nickel (NOVAMET, 60 wt.% Ni) with average dimensions of 75–120 μm were introduced into liquid matrix alloy through mechanical mixing. Near-eutectic AlSi12CuNiMg alloy constituting the matrix of composite to be tested was used as a comparative material. The tests were performed on raw specimens (not subjected to heat treatment). The chemical composition of AlSi12CuNiMg alloy is presented in **Table 1**.

Disc shaped specimens with a diameter of 25 mm and thickness of 6 mm were used for tribological tests. Three (n=3) specimens from each test material group were used for wear test. The specimens were subjected to grinding on water abrasive papers with grains size of 220, 600 and 1200, sequentially. Then the specimens

Table 1. The chemical composition of AlSi12CuNiMg aluminium cast alloy in accordance with PN-76/H-88027 standard (wt.%) [L. 17]

Tabela 1. Skład chemiczny odlewniczego stopu aluminium AlSi12CuNiMg wg normy PN-76/H-88027 **[L. 17]**

Si	Mg	Cu	Fe	Ni	Mn	Ti	Zn	Al
11.5–13	0.8–1.5	0.8–1.5	0.6–0.8	0.8–1.3	0.2	0.1	0.2	bal.

were subjected to mechanical polishing by means of a suspension of diamond particles (3 μm), a suspension of oxides particles (0.05 μm), washed with acetone, and dried in a warm air stream thereafter. The roughness Ra of the materials subjected to polishing reached level Ra≈0.05 μm. Surface preparation of the samples was dictated by the desire to obtain accurate results when determining the wear factor (according to ASTM G40) on the basis of measurements of profilometric wear volume.

Wear tests were completed on a ball-on-disc tribometer manufactured by CSM Instruments. Dry sliding wear tests were conducted according to the ASTM G99-95c **[L. 18]** and DIN 50 324 standard **[L. 19]**. Balls with a diameter of 6 mm made of 100Cr6 steel with hardness of 64HRC (manufactured by CSM Instruments) were used as a counter-specimen (ball). Counter-specimen materials were selected for the ball-on-disc tests, but only the disc wear results were studied during the wear test **[L. 15, 20]**. The tests were carried out at the load of 5N and a linear speed of 0.035 m/s on the radius of 5.5 mm. The total test travel used to record the variation of friction coefficient was equal to 100 m. Volume loss of specimens in the form of wear trace created as a result of specimen and counter-specimen mating was used as the wear measurement. Therefore, the surface area of specimen wear profile was measured by means of Dektak 150 contact profilometer (manufactured by Veeco Instruments) along specimens' circumferences (in 12 places, the sample rotating 30 deg.). The radius of the measuring needle was equal to 2 μm. The wear volume was determined as the product of the average value of specimen wear surface area and the circumference of wear trace circle created in ball-on-disc test. Then, the wear factor (K) was determined by means of the following equation, considering the value of wear volume, applied force, and sliding distance used in course of tests:

$$K = \frac{Wear\ volume}{Applied\ force \times sliding\ distance}\left[m^3 N^{-1} m^{-1}\right] \quad (1)$$

Phenom ProX scanning microscope (manufactured by Phenom-World B.V.) with EDS detector was used for the analysis of the microstructure of tested materials.

RESULTS AND DISCUSSION

The microstructure of AlSi12CuNiMg alloy is characterized by the presence of needle–shaped α(Al)+β(Si) eutectic uniformly distributed in the background of solid Si solution in aluminium α(Al) (**Fig. 1a**). The intermetallic phases, i.e. Al(CuNi)Si and Mg_2Si, occur as a result of the additions of copper, nickel, and magnesium. Their presence was detected based on the executed point microanalysis using EDS analysis described in a more detailed manner in [**L. 21**]. Konečná et al. **[L. 2]** emphasize that eutectoid alloy AlSi12CuNiMg is characterized by the presence of intermetallic phase Al(CuNi)Si. However, published data **[L. 22, 23]** indicate that, in the case of Al-Si-Cu-Mg casting alloys, high copper concentration in α-phase contributes to Al_2Cu precipitations.

The Mg_2Si phase is observed in the alloy microstructure in the form of specific precipitations, i.e. so called "Chinese writing." Near-eutectic silumin microstructure is also characterized by bright precipitations characterized by specific branched shape. Their point microanalysis indicates the presence of an AlSiFeNi phase with a complex chemical composition without a determined chemical formula. Its presence is possible due to the presence of iron and nickel in this alloy. Intermetallic phases are situated mainly in eutectic mixture α(Al)+β(Si).

However, the structure of AlSi12CuNiMg/5.7 wt.% Gr composite is characterized by the presence of α(Al)+β(Si) eutectic mixture and particles of graphite reinforcing phase, and the precipitations of intermetallic phases are visible in the background of solid Si solution in aluminium α(Al) (**Fig. 1b**). Si precipitations in eutectic mixture α(Al)+β(Si) are needle shaped and are uniformly distributed in the matrix alloy structure. The structure of bonding between aluminium alloy and graphite particles seems to be correct. Microscopic observations do not indicate the presence of any reaction products in the matrix / reinforcement bonding structure resulting from their interaction in the course of composite material synthesis. We did find porosity and other structural discontinuities in the composite microstructure. Moreover, the structure of composite material contains an intermetallic phase Al_3Ni characterized by an elongated shape and distributed in solid Si solution in aluminium. Additionally, there are precipitations of a specific Mg_2Si phase ("Chinese script") located in α(Al)+β(Si) eutectic mixture. X-Ray EDS point analysis in selected micro-areas indicates the presence of intermetallic phases (in trace amounts) containing, Si, iron, copper and nickel (not including Al). Similarly as in the case of AlSi12CuNiMg alloy constituting the matrix of composite, the AlSiFeNi phase precipitation takes place as a result of alloy contamination with iron.

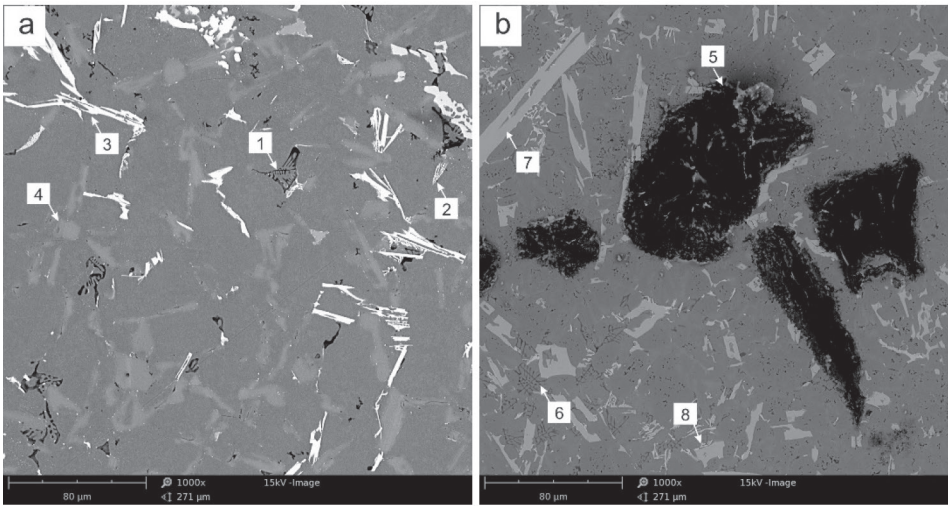

Fig. 1. Microstructure examined by SEM and EDS. Phases characteristics in cast: a) AlSi12CuNiMg, b) AlSi12CuNiMg/5.7 wt.% Gr. Legend: 1 – Mg_2Si (spectrum wt. %: 51.2Al, 26.4Mg, 22.4Si), 2 – Al(CuNi)Si (spectrum wt. %: 75.4Al, 11.8Cu, 7.1Si, 5.7Ni), 3 – AlSiFeNi (spectrum wt. %: 69.6Al, 14.9Ni, 12.1Si, 3.3Fe), 4 – Si (spectrum wt. 71.6Si, 28.4Al), 5 – graphite particle (spectrum wt. %: 96.lC, 3.9Si), 6 – Mg_2Si (spectrum wt. %: 61.1Al, 21.5Mg, 17.4Si), 7 – Al_3Ni (spectrum wt. %: 74.1Al, 19.1Ni, 6.7Si), 8 – AlSiFeNi (spectrum wt. %: 73.7Al, 13.4Ni, 7.4Si, 3.3Fe)

Rys. 1. Mikrostruktura badana przy użyciu SEM i EDS. Charakterystyczne fazy w odlewie: a) AlSi12CuNiMg, b) AlSi12CuNiMg/5,7 wt.% Gr. Legenda: 1 – Mg_2Si (widmo wt. %: 51,2Al, 26,4Mg, 22,4Si), 2 – Al(CuNi)Si (widmo wt. %: 75,4Al, 11,8Cu, 7,1Si, 5,7Ni), 3 – AlSiFeNi (widmo wt. %: 69,6Al, 14,9Ni, 12,1Si, 3,3Fe), 4 – Si (widmo wt. %: 71,6Si, 28,4Al), 5 – cząsteczka grafitu (widmo wt. %: 96,lC, 3,9Si), 6 – Mg_2Si (widmo wt. %: 61,1Al, 21,5Mg, 17,4Si), 7 – Al_3Ni (widmo wt. %: 74,1Al, 19,1Ni, 6,7Si), 8 – AlSiFeNi (widmo wt. %: 73,7Al, 13,4Ni, 7,4Si, 3,3Fe)

The values of recorded friction coefficients are specified in **Table 2,** and **Figure 2** illustrates the graphical interpretation vs. distance. Comparative analysis of friction coefficients demonstrated that the composite material is characterized by a lower average value ($\mu = 0.440$) than the matrix material ($\mu = 0.483$). Initially higher values of friction coefficients are caused by the fact that the peaks of the roughness profile undergo shearing, and the plastic deformation of matrix takes place thereafter. Shearing of the peaks of the roughness profile is closely related to the presence in the structure of needle–shaped α(Al)+β(Si) eutectic. During sample preparation (polishing), plastic matrix α(Al) is more susceptible to abrasion than grains of silicon, which protrude above the zero profile disc. Therefore, in the initial phase of wear testing, there is shearing of the peaks of the roughness profile. After the grinding process on the sliding surface, the contact surface area between mating surfaces is increased, and the value of friction coefficient is reduced and stabilized. The lower value of friction coefficient is associated with the presence of a graphite film created between mating sliding pairs.

Table 2. Summary of friction coefficients determined for tested material mating with a counter-specimen made of steel 100Cr6

Tabela 2. Zestawienie wyznaczonych współczynników tarcia badanych materiałów we współpracy z przeciwpróbką ze stali 100Cr6

Sample material	Average friction coefficients μ	Standard deviation
AlSi12CuNiMg	0.483	0.069
AlSi12CuNiMg/5.7 wt.% Gr	0.440	0.029

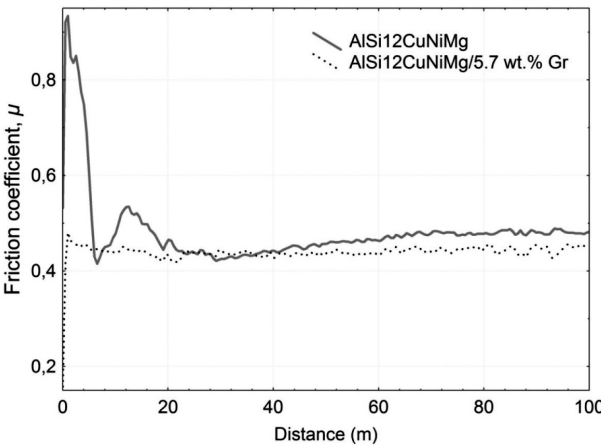

Fig. 2. The curve illustrating variations of friction coefficient vs. distance at the load of 5N

Rys. 2. Wykres ilustrujący zmiany współczynnika tarcia w funkcji drogi przy obciążeniu 5N

The tests **[L. 15, 24]** that the reinforcement of aluminium alloys by means of graphite particles results in the generation of a permanent thin and lubricating graphite layer on sliding surface is a "film," which reduces the value of friction coefficient and thus reduces Al/Gr composites wear. According to data **[L. 25]**, the value of friction coefficient decreases with increase of weight percentage of graphite particles up to 3-5%. A further increase of the weight percentage of graphite particles does not contribute to the reduction of friction coefficient. The value of the weight percentage of graphite reduces the abrasive wear of composite to 20% of matrix wear. A similar opinion has been expressed by Ted Guo and Tsao **[L. 24]** who found no significant influence of increased percentage from 5 to 8% Gr on the reduction of the friction coefficient. The analysis of experimental results executed by Rohatgi et al. **[L. 26]** also confirms that the value of friction coefficient in graphite-reinforced composites is significantly lower in comparison to the matrix material. Moreover, they indicate that, in the case of graphite content in composite exceeding 20% v/v, the value of friction coefficient is similar to its value for pure graphite and is independent of matrix material. Furthermore, the presence of graphite particles in the matrix of aluminium alloys increases its seizing resistance. Therefore, the operation in boundary lubrication conditions is possible without seizing.

In case of AlSi12CuNiMg, a higher value of friction coefficient is associated with the plastic deformation of soft matrix wear track or with loose rolling of hard particles originating from secondary wear. Si precipitations constitute a natural obstacle for counter-specimen material. In the course of the test duration (after certain period of time), Si particles are separated and the wear process is intensified as a result of additional interaction between particles and sliding surfaces. Such behaviour results in an increased abrasive wear effect in alloys being tested or in loose rolling of hard Si particles between mating surfaces of the specimen and counter-specimen. This behaviour has been observed in the case of wear of AlSi9Mg alloy **[L. 6]**. In such a case, the scratches on the surface of mating specimen or plastic deformation of solid solution α(Al) can be caused by rolling particles leaving specific traces in the form of grooves. However, in the case of a composite, the thin graphite layer is broken.

The analysis of cross-section profiles of wear tracks (**Fig. 3**) showed piles on the borders of wear tracks edges. Higher piles on the borders are observed for AlSi12CuNiMg alloys constituting composite matrix. Furthermore, the depth of the lateral profile of the wear trace for graphite reinforced composite is almost half the value of this profile of AlSi12CuNiMg alloy. Additionally, ridging traces on the bottom of composite wear track are less advanced than in case of AlSi12CuNiMg alloy. The lateral profile of specimens' wear trace indicates a higher wear of material constituting the matrix.

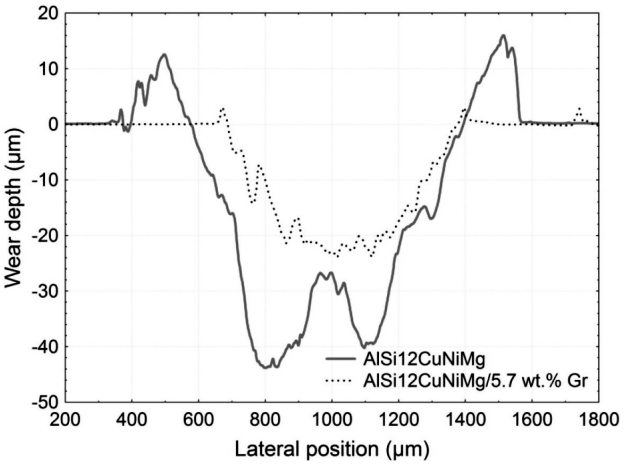

Fig. 3. Typical cross-section profiles of wear tracks
Rys. 3. Typowe profile (przekrój poprzeczny) śladów zużycia

Figure 4 illustrates the results of wear volume for materials being tested. It has been observed that the wear resistance of composite material AlSi12CuNiMg/5.7 wt.% Gr was about 46% higher than in the case of material constituting the matrix in comparative tests.

In order to verify whether obtained changes are statistically significant, the STATISTICA program was used for analysis encompassing parametric tests for independent samples. Statistical analysis carried out by means of Shapiro-Wilk tests for wear factor measurement showed that the obtained results have a normal distribution $p>0.05$ (assuming $\alpha=0.05$). Therefore, $p>\alpha$, and there are no grounds to reject the hypothesis on the normal distribution of the feature being examined. This can be a sign of a high structural uniformity of materials being examined. T-Student test (for $\alpha=0.05$) showed that wear differences are statistically significant $p=0.009$ (i.e. $p<0.05$).

The microscopic observations of wear traces showed that, in the case of matrix AlSi12CuNiMg

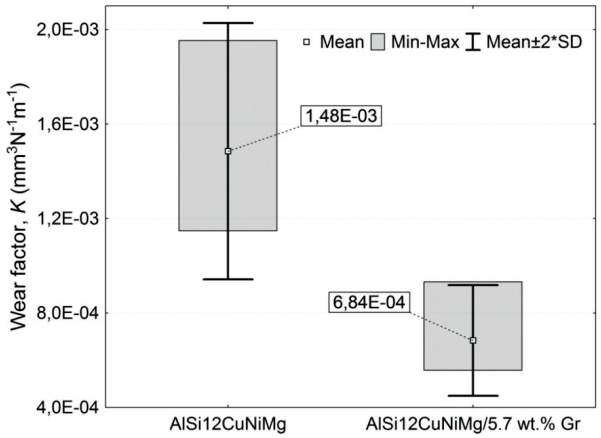

Fig. 4. Diagram illustrating wear factor *K* for tested materials
Rys. 4. Wykres ilustrujący współczynnik zużycia K dla badanych materiałów

material constituting the matrix, track edges are irregular and that plastic deformations are present (**Fig. 5a**) and that the created wear track is significantly wider than in the case of composite (**Fig 5b**). However, the width of the composite wear trace is more uniform along the whole circumference. Moreover, the distribution of reinforcing graphite phase particles is uniform in the whole structure.

SEM analysis of wear tracks (**Fig. 6**) indicates that abrasive wear is the prevailing mechanism in the both cases. The micro-cutting process is an intensifying factor. Wear traces in the form of continuous cracks resulting from moving products originating from secondary wear are present along wear tracks. Furthermore, these materials are characterized by the presence of a plastic zone associated with material accumulation along counter-specimen movement. Abrasion and groove forming (particularly in the case of AlSi12CuNiMg alloy) was the prevailing mechanism. Additionally, wear traces were characterized by specific micro-cracks perpendicular to the movement direction, which indicates to the presence of fatigue wear. As a result of multiple upsetting of the same material volume by means of counter-specimen, low cycle fatigue phenomenon occurs and delaminations of the aluminium matrix are observed. In the case of a sufficient degree of plastic deformation at upsetting of matrix material, it is possible to describe the material delamination process by means of the Suh model **[L. 27]**. Except for the delamination phenomena, hard Si particles are eliminated by abrasive mechanisms, consequently leading to significant plastic deformation. Furthermore, the authors emphasize that it is possible to reduce the degree of matrix material wear due to the possibility of the formation of oxides performing the role of grease. Moreover, oxides particles accumulating along the wear track valleys are removed in course of

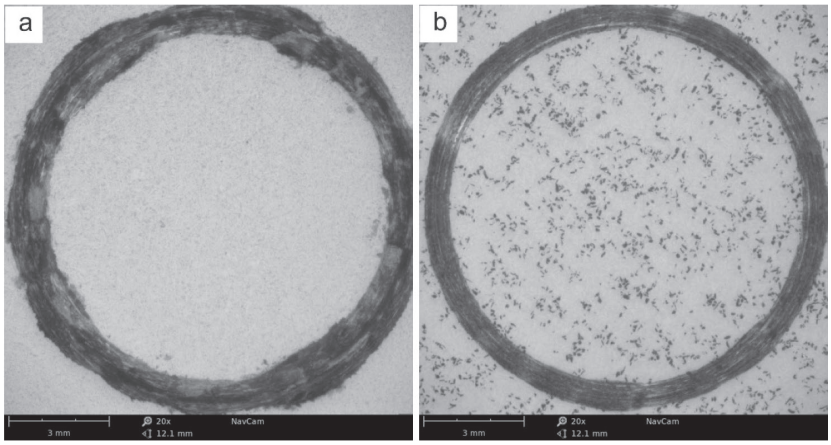

Fig. 5. Photographs of sample (disc) surfaces after wear test: (a) AlSi12CuNiMg alloy, (b) AlSi12CuNiMg/5.7 wt.% Gr composite

Rys. 5. Fotografie powierzchni próbek (dysków) po teście zużycia: (a) stop AlSi12CuNiMg, (b) kompozyt AlSi12CuNiMg/5,7 wt.% Gr

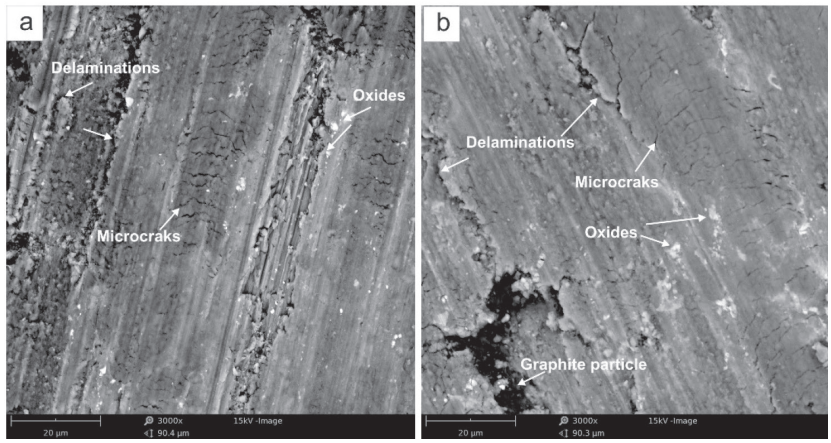

Fig. 6. SEM microphotographs of the worn surfaces of: a) AlSi12CuNiMg alloy, and b) AlSi12CuNiMg/5.7 wt.% Gr composite

Rys. 6. Mikrofotografie SEM zużytych powierzchni: a) stopu AlSi12CuNiMg, b) kompozytu AlSi12CuNiMg/5,7 wt.% Gr

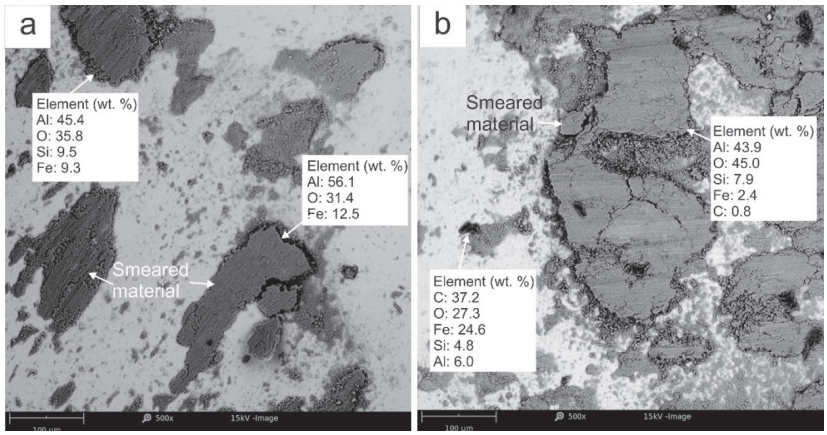

Fig. 7. SEM images showing the smeared layer and its EDS analysis of the ball surface after wear test of: a) AlSi12CuNiMg alloy, and b) AlSi12CuNiMg/5.7 wt.% Gr composite

Rys. 7. Obrazy SEM ilustrujące zasmarowaną warstwę i analizy EDS powierzchni kulki po testach zużycia: a) stopu AlSi12CuNiMg, b) kompozytu AlSi12CuNiMg/5,7 wt.% Gr

counter-specimen movement. This phenomenon is confirmed by research **[L. 10, 12]**.

In order to evaluate the wear mechanism of materials tested, the SEM images and EDS analyses were also acquired from the ball surface after the wear test (**Fig. 7**). The figure shows that the ball surface was partially covered by transferred materials. The surfaces of the balls are characterized by extensive smearing. However, smearing appears to be next to the abrasion dominant wear mechanism for all materials tested. Adhesive tacking of steel with aluminium matrix fragment occurs and consequently leads to its pulling out, which is observed as "smearing over" of the matrix on the ball surface, as confirmed by the authors of publication **[L. 20]**. EDS analysis show that the chemical compositions of balls' surface due to wear consists of a mixture of Al, Si, O, and a little Fe. In addition to these elements, in the case of the tribological pair of steel-composite, graphite particles were found on the ball's surface (**Fig. 7b**). As shown by the literature **[L. 15, 24],** during tribological processes after a given period of time between the counter-sample and the surface of the sample, a graphite film can then be created.

SUMMARY

Microscopic observations showed the uniform distribution of the graphite-reinforcing phase in the composite structure, and the structure of bonding between aluminium matrix and graphite particles seems to be correct.

Graphite particles cause a significant reduction in the coefficient of friction in the initial phase of the tribological tests. The friction coefficients after a distance of 20 m of all materials show similar trends. They are stabilized by following an initial decrease as the sliding distance increases. This can be attributed to the formation of a stable tribo-layer on the wear surface of the alloys. Comparative analysis of friction coefficients showed that composite material is characterized by a lower average value (μ=0.440) than the matrix material (μ=0.483). It has been observed that wear resistance of composite material AlSi12CuNiMg/5.7 wt.% Gr was about 54% higher than in the case of material constituting the matrix in comparative tests. The differences in the wear factors are statistically significant.

Wear type in the both materials being tested indicates a typical abrasive wear mechanism intensified by micro-cutting. Lateral micro-cracks are the symptoms of simultaneously occurring fatigue wear. Other wear mechanisms, i.e. delaminations and oxidation, have also occurred. In addition, there are adhesive phenomena associated with the transfer of mixture of Al, Si, and O (C in the case of composite) on the surface of steel 100Cr6.

REFERENCES

1. Dwivedi D.K., Adhesive wear behaviour of cast aluminium–silicon alloys: Overview, Materials and Design, 31 (5), 2010, 2517–2531.
2. Konečná R., Nicoletto G., Kunz L., Svoboda M., Bača A., Fatigue strength degradation of AlSi12CuNiMg alloy due to high temperature exposure: a structural investigation, Procedia Engineering, 74, 2014, 43–46.
3. Chandrashekharaiah T.M., Kori S.A., Effect of grain refinement and modification on the dry sliding wear behaviour of eutectic Al–Si alloys, Tribology International, 42 (1), 2009, 59–65.
4. Bieniaś J., Walczak M., Surowska B., Sobczak J., Microstructure and corrosion behaviour of aluminium fly ash composites, Journal of Optoelectronics and Advanced Materials, 5 (2), 2003, 493–502.
5. Devaraju A., Kumar A., Kotiveerachari B., Influence of addition of Gr_p/Al_2O_{3p} with SiC_p wear properties of aluminum alloy 6061-T6 hybrid composites via friction stir processing, Transactions of Nonferrous Metals Society of China, 23 (5), 2013, 1275−1280.
6. Walczak M., Pieniak D., Zwierzchowski M., The tribological characteristics of SiC particle reinforced aluminium composites, Archives of Civil and Mechanical Engineering, 15 (1), 2015, 116−123.
7. Yang J.B., Lin C.B., Wang T.C., Chu H.Y., The tribological characteristics of A356.2Al alloy/$Gr_{(p)}$ composites, Wear, 257 (9-10), 2004, 941–952.
8. Rohatgi P.K., Cast Metal-Matrix Composites, ASM Handbook. Casting, ASM International, 1992, 1840–1872.
9. Krishnan B.P., Raman N., Narayanaswamy K., Rohatgi P.K., Performance of an Al-Si-graphite particle composite piston in a Diesel engine, Wear, 60 (1), 1980, 205–215.
10. Omrani E., Moghadam A.D., Algazzar M., Menezes P.L., Rohatgi P.K., Effect of graphite particles on improving tribological properties Al-16Si-5Ni-5Graphite self-lubricating composite under fully flooded and starved lubrication conditions for transportation applications, The International Journal of Advanced Manufacturing Technology, 87(1), 2016, 929–939.
11. Riahi A.R., Alpas A.T., The role of tribo-layers on the sliding wear behaviour of graphitic aluminum matrix composites, Wear, 251 (1-12), 2001, 1396–1407.
12. Prabhudeva M.S., Auradi V., Venkateswarlu K., Siddalingswamy N.H., Kori S.A., Influence of Cu addition on dry sliding wear behaviour of A356 alloy. Procedia Engineering, 97, 2014, 1361–1367.

13. Sharma R., Anesh, Dwivedi D.K., Influence of silicon (wt.%) and heat treatment on abrasive wear behaviour of cast Al–Si–Mg alloys, Materials Science and Engineering: A, 408 (1-2), 2005, 274–280.
14. [Mahato A., Verma N., Jayaram V., Biswas S.K., Severe wear of a near eutectic aluminium–silicon alloy, Acta Materialia, 59 (15), 2011, 6069–6082.
15. Rajaram G., Kumaran S., Srinivasa Rao T., Kamaraj M., Studies on high temperature wear and its mechanism of Al–Si/graphite composite under dry sliding conditions, Tribology International, 43 (11), 2010, 2152–2158.
16. Rudnik D., Sobczak J., Wojciechowski A., Pietrzak K., New material solutions in combustion engines, Journal of KONES Internal Combustion Engines, 10 (3-4), 2003, 303–313.
17. PN-76/H-88027, Casting aluminium alloys. Grade. Polish Committee for Standardization, UKD 669.715.018.28, Warsaw, Poland 1976.
18. ASTM G99-95c; Standard test method for wear testing with a Pin-on-Disc apparatus.
19. DIN 50 324; Testing of Friction and Wear.
20. Alemdag Y., Beder M., Microstructural, mechanical and tribological properties of Al-7Si-(0-5)Zn alloys, Materials and Design, 63, 2014, 159-167.
21. Bieniaś J., The anlysis of the infuence of ceramic phase and matrix structure on corrosion resistance of Al-Si composites with dispersed graphite reinforcement [dissertation]. University of Technology, Lublin, 2010.
22. Wang G., Bian X., Wang W., Zhang J., Influence of Cu and minor elements on solution treatment of Al–Si–Cu–Mg cast alloys, Materials Letters, 57 (24-25), 2003, 4083–4087.
23. Sjölander E., Seifeddine S., The heat treatment of Al–Si–Cu–Mg casting alloys, Journal of Materials Processing Technology, 210 (10), 2010, 1249–1259.
24. Ted Guo M.L., Tsao C.-Y.A, Tribological behaviour of self-lubricating aluminium/SiC/graphite hybrid composites synthesized by the semi-solid powder-densification method, Composites Science and Technology, 60 (1), 2000, 65–74.
25. Gibson P.R., Clegg A.J., Das A.A., Wear of cast Al-Si alloys containing graphite, Wear 95 (2), 1984, 193–198.
26. Rohatgi P.K., Ray S., Liu Y., Tribological properties of metal matrix-graphite particle composites, International Materials Reviews, 37 (1), 1992, 129–152.
27. Suh N.P., An overview of theory of wear, Wear, 44 (1), 1977, 1–16.